Bound states of a finite periodic potential

D. W. L. Sprung, J.D. Sigetich and Hua Wu
Department of Physics and Astronomy, McMaster University, Hamilton, Ontario L8S 4M1 Canada

and J. Martorell
Departament d'Estructura i Constituents de la Materia, Facultat Física, University of Barcelona, Barcelona 08028, Spain

(November 2, 1999)

We locate the bound states for a one-dimensional potential which consists of N identical cells, by the transfer matrix method. Our expressions involve only the Bloch phase and a scattering phase, both of which are properties of the single cell. The method applies to an arbitrary but non-overlapping potential shape, and thereby emphasizes generic properties over specific details. It gives useful qualitative insight without tedious calculations. We discuss the evolution of the bound states as the inter-cell spacing is varied, and the occurrence of surface states as bound states in a forbidden zone.

PACS number(s): 03.65.Db, 03.65.Nk, 73.20.Dx

I. INTRODUCTION

A course on quantum mechanics usually begins with the bound states of a potential well, followed by tunnelling through a barrier. The case of a double barrier is often included and resonances related to quasi-bound states trapped between the two barriers are discussed. Sometimes the related situation of a double potential well is used to illustrate the development of even and odd parity bound states as the separation between the wells is reduced.

We have found a nice way to discuss the bound states of a variable number N of identical potential wells, based on the transfer matrix method as developed in our earlier paper [1]. It shows how the states of the finite periodic system evolve from those of the separate wells, as well as the symmetries of the resulting wave functions. It also shows how the system evolves as the number of wells increases $N = 1, 2, 3 \cdots$. Further, many of the results can be followed without detailed calculations.

The infinite periodic array is of course the famous Kronig-Penney model [2] of a crystal. In recent years experiments on heterostructures have lead to greater interest in the case of finite and not very large N [3–10]. The limit $N \to \infty$ is also a subject of some discussion [11,12]. Our method was developed in this context. The closest parallel to our treatment is in the excellent book by Cohen-Tannoudji et al. [13].

Starting with N *widely* separated potential wells, for each single-well bound state, one has exactly N degenerate bound states. These are either the individual states in each separate well, or any N linear combinations of them. However, as the separation distance ℓ between the wells is decreased, this degeneracy is broken, and specific combinations are selected as the eigenstates. Evolving from the most deeply bound level of the single well, the most symmetric state will have a positive amplitude in each well, and the most antisymmetric state will have alternating signs between adjacent wells. The resulting nodes push up the kinetic energy and reduce the binding. At some value of separation ℓ the least bound state may become unbound. When the wells finally touch, one can in principle have as few as just one bound state remaining, depending on the strength of the individual well. We will trace this evolution.

Following a brief resume of the transfer matrix method, we apply it to bound states in section 2. In sections 3 and 4 we apply the method to specific examples where one has analytic results. These are the row of several delta-functions and the row of square wells. We discuss the evolution of the spectrum as the inter-cell distance is varied in section 5. In section 6 we give examples of surface states while Section 7 contains the summary and conclusions.

II. TRANSFER MATRIX METHOD AND BOUND STATES

In an earlier paper [1] we considered scattering in one-dimension by a finite periodic potential which consists of N identical cells. The potential within a cell is real but otherwise arbitrary, and outside the array is for simplicity taken to be a constant which we can define to be the zero of energy. Time reversal symmetry holds. At positive energies $E = \hbar^2 k^2/2m$, the scattering properties of a single cell are subsumed in the transmission $t(k)$ and reflection $r(k)$ amplitudes from which the transfer matrix is constructed in the form [1]

$$\mathbf{M} = \begin{pmatrix} \frac{1}{t(k)} & \frac{r^*(k)}{t^*(k)} \\ \frac{r(k)}{t(k)} & \frac{1}{t^*(k)} \end{pmatrix} \tag{1}$$

In our representation, the wave function is expressed (in a translation invariant way) in terms of right and left moving waves on each side of the cell,

$$\begin{aligned} \Psi(x) &= f_1(k,x)e^{ik(x-x_\alpha)} + f_2(k,x)e^{-ik(x-x_\alpha)} \\ \Psi'(x) &= ikf_1(k,x)e^{ik(x-x_\alpha)} - ikf_2(k,x)e^{-ik(x-x_\alpha)} \end{aligned} \tag{2}$$

and the amplitudes on opposite boundaries of a cell at $x_\alpha = x_L, x_R$, are related by

$$\begin{pmatrix} f_1 \\ f_2 \end{pmatrix}_L = \begin{pmatrix} M_{11} & M_{12} \\ M_{21} & M_{22} \end{pmatrix} \begin{pmatrix} f_1 \\ f_2 \end{pmatrix}_R \tag{3}$$

For example if the incident wave is from the left, then the f_i are related to the transmission and reflection amplitudes as follows:

$$\begin{pmatrix} f_1 \\ f_2 \end{pmatrix}_L = \begin{pmatrix} 1 \\ r(k) \end{pmatrix} \qquad \begin{pmatrix} f_1 \\ f_2 \end{pmatrix}_R = \begin{pmatrix} t(k) \\ 0 \end{pmatrix} \quad . \tag{4}$$

Substituting these into eq. 3 determines the first column of elements of the transfer matrix as shown in eq. 1. Denoting the amplitudes for waves incident from the right as r', t', one easily finds that $M_{12} = -r'/t'$. For a time reversal invariant system, the amplitudes for incident waves from the right are related to those from the left by $t' = t(k)$, and $r'/t' = -r^*(k)/t^*(k)$. Conservation of flux, which makes $\det M = 1$, then determines $M_{22} = 1/t^*(k)$. This justifies eq. 1 for real values of k. If in addition the unit cell is reflection invariant, then $r' = r(k)$, making the off-diagonal elements of M pure imaginary.

The cell width is denoted as d, so $x_R = x_L + d$. Here we consider only potentials that are non-zero over a finite width $2b$. The potential may be zero over a (variable) part of the cell width denoted as ℓ, so $d = 2b + \ell$. By varying ℓ, one changes the spacing between the potential wells. We do not consider overlapping potentials here, so ℓ is never negative. Changing ℓ alters the phases of the amplitudes t, r but does not change their absolute values in the physical scattering region. It is convenient to add the extra space symmetrically on each side of the unit cell, so as to preserve reflection symmetry *if* it exists. Then we have the relation

$$\begin{aligned} &\mathbf{M}(d) = \\ &\begin{pmatrix} e^{-ik\ell/2} & 0 \\ 0 & e^{+ik\ell/2} \end{pmatrix} \mathbf{M}(2b) \begin{pmatrix} e^{-ik\ell/2} & 0 \\ 0 & e^{+ik\ell/2} \end{pmatrix} \\ &= \begin{pmatrix} e^{-ik\ell}M_{11}(2b) & M_{12}(2b) \\ M_{21}(2b) & e^{+ik\ell}M_{22}(2b) \end{pmatrix} \end{aligned} \tag{5}$$

For a system of N-cells, the transfer matrix is simply the product $\mathbf{M}^N$, whose elements will be distinguished by a superscript N. Unitarity gives $\det(\mathbf{M}) = 1$, and therefore one has the relation

$$\mathbf{M}^2 = (2\cos\phi)\mathbf{M} - \mathbf{I} \tag{6}$$

where the Bloch phase ϕ is defined by $2\cos\phi = \mathrm{Tr}(\mathbf{M})$. By induction one proves [14] that

$$\mathbf{M}^N = \frac{\sin N\phi}{\sin\phi}\mathbf{M} - \frac{\sin(N-1)\phi}{\sin\phi}\mathbf{I} \tag{7}$$

From this, it is clear that the transfer matrix for a single cell plus the Bloch phase directly determines the scattering properties of an N-cell system. For example, $M_{21}^N = r_N/t_N$, the ratio of reflection and transmission amplitudes for N-cells. Using eq. 7 gives the very useful result [14]

$$\frac{1}{|t_N|^2} - 1 = \frac{\sin^2 N\phi}{\sin^2\phi}\left(\frac{1}{|t_1|^2} - 1\right) \quad . \tag{8}$$

This shows that whenever the single cell is transparent ($|t_1|^2 = 1$), so are N-cells. But in addition within each allowed band where ϕ increases by π, there are $N-1$ points $\phi_j = j\pi/N$, $j = 1, 2, ...(N-1)$ which also give perfect transmission.

Bound states may be considered as a special case of the scattering problem, where there is no incoming wave on either side of the system, only outgoing waves:

$$\begin{pmatrix} 0 \\ f_2 \end{pmatrix}_L = \begin{pmatrix} M_{11}^N & M_{12}^N \\ M_{21}^N & M_{22}^N \end{pmatrix} \begin{pmatrix} f_1 \\ 0 \end{pmatrix}_R \tag{9}$$

and occur when $M_{11}^N = 0$. (Virtual or anti-bound states correspond to $M_{22}^N = 0$.) This is consistent with a bound state being a pole of the scattering amplitude $t(k)$. We follow the usual convention that $k \to i\kappa$ at negative energies, so the bound state poles occur on the positive imaginary axis in the momentum (k) plane. The outgoing wave then becomes a decaying exponential on both sides of the array.

From eq. 1 we have $\cos\phi = ReM_{11}$ above threshold. Below threshold, the channel wave number becomes complex: $k \to i\kappa$, so incoming/outgoing waves become exponentially increasing/decreasing (in direction away from the cell) waves. When we analytically continue the elements of $\mathbf{M}$ onto the imaginary axis, they become real numbers, but this does *not* mean that the diagonal elements of M become equal. Rather, it turns out that $M_{11}(\kappa) = M_{22}(-\kappa)$. The symmetry which is preserved is time-reversal: interchanging the channel labels and the direction of the waves leaves the matrix invariant. (See eq.19 below for an example). So both diagonal elements are required to compute $\cos\phi$, below threshold.

The condition for bound states of an N-cell system, $M_{11}^N = 0$, can be rewritten in several useful forms. Using eq. 7, we have

$$\begin{aligned} M_{11}^N \sin\phi &= M_{11}\sin N\phi - \sin(N-1)\phi \\ &= \sin N\phi(M_{11} - \cos\phi) + \cos N\phi\sin\phi \\ &\equiv A(k)\sin(N\phi + \delta) \end{aligned} \tag{10}$$

where the phase δ is defined ($0 \leq \delta \leq \pi$) by

$$\begin{aligned} \tan\delta &= \frac{\sin\phi}{M_{11} - \cos\phi} \quad \text{and} \\ A^2(k) &= (M_{11})^2 - 2\cos\phi M_{11} + 1 \\ &= 1 - M_{11}M_{22} = -M_{12}M_{21} \end{aligned} \tag{11}$$

gives the amplitude $A(k)$, which can vanish only when we are dealing with a diagonal M matrix, with $M_{11} = e^{\pm i\phi}$. Obviously this cannot be at a bound state of the single cell system which requires $M_{11} = 0$, and $A^2 = 1$. If $A(k)$ were to vanish in the allowed band, then that energy would give a bound state for all N including $N = 1$, in contradiction to the last statement. Hence, using eq. 10, the condition for a bound state of the N-cell system, in an allowed band, becomes

$$\chi_N \equiv N\phi + \delta = j\pi \quad , \quad j = 1, 2, ... \tag{12}$$

Within an allowed band, ϕ varies by π, so χ_N varies by $N\pi$ plus the change in δ over the band. From a plot of χ_N over the band one can read off the bound state energies as seen for example in Figs. 2 and 4 below. The number of bound states will depend on how δ behaves. For example, consider the hypothetical situation where $M_{11} = M_{22} = \cos\phi$, which would make $\delta = \pi/2$. Then the bound-state condition would be

$$\cos N\phi = 0 \tag{13}$$

with N solutions at $\phi_j = (j - 1/2)\pi/N$, $j = 1, 2, ...N$, in an allowed zone where ϕ varies from zero to π. In general, however, δ is not a constant and is not equal to $\pi/2$, but so long as δ increases over the band, we expect to have N solutions at positions within the strips of width π/N about the points ϕ_j. When N is large these strips are narrow, and this may already provide useful information.

One point to notice is that M_{11}^N is independent of the sign of ϕ, because it involves the ratio of two sine-functions. In the physical region ϕ starts at some initial value, usually zero, and it increases from there to π in the first allowed band, to 2π in the second, and so on. (An allowed band is one where ϕ is a real angle.) The sign of the cosine plays a vital role in all this, but it would change nothing if we had used $-\phi$ everywhere. On the other hand, the *relative sign* of δ and ϕ is important, and this is set by the sign of $M_{11} - \cos\phi = \frac{1}{2}(M_{11} - M_{22})$ in the denominator in the first line of eq. 11.

In the above, we have assumed that ϕ is a real angle. Below threshold, M_{ij} are real, but there is nothing to prevent $|\cos\phi| > 1$. This is a "forbidden zone", in which $\phi \to i\theta + p\pi$, with $p =$ even when $\cos\phi > 1$ and $p =$ odd when $\cos\phi < -1$ [1]. Repeating the above arguments, and replacing $\delta \to i\eta$ gives

$$M_{11}^N \sinh\theta = (-)^p A(k) \sinh(N\theta + \eta) \tag{14}$$

where

$$\begin{aligned} \tanh\eta &= \frac{\sinh\theta}{(-)^p M_{11} - \cosh\theta} \quad \text{and} \\ A^2(k) &= (M_{11})^2 - 2(-)^p \cosh\theta M_{11} + 1 \\ &= 1 - M_{11}M_{22} = -M_{12}M_{21} \end{aligned} \tag{15}$$

As before, the amplitude can vanish only when we are dealing with a diagonal M matrix, with $M_{11} = (-)^p e^{\pm\theta}$. Because $\cosh\theta$ is always positive, the parameter p has been introduced to take care of the sign. For the same reasons discussed earlier, the relative sign of θ and η is determined by the denominator of eq. 15. The only way to have a zero of M_{11}^N is to have a cancellation between $N\theta$ and η in the argument of the hyperbolic sine in eq.14. It requires *opposite* signs of θ and η for this to occur.

To shed some further light, note that eqs. 10, 14 can be put in the alternative forms

$$\begin{aligned} M_{11}^N &= \cos N\phi + \frac{\sin N\phi}{\tan\delta} \\ &= \frac{1}{\sin\delta} \sin(N\phi + \delta) \\ &= (-)^p \big(\cosh N\theta + \frac{\sinh N\theta}{\tanh\eta}\big) \\ &= (-)^p \frac{1}{\sinh\eta} \sinh(N\theta + \eta) \end{aligned} \tag{16}$$

depending on whether one deals with the case of real ϕ or imaginary $\phi \to i\theta + p\pi$.

For the imaginary case, line four is most helpful. Suppose that θ is positive. In some cases, $\tanh\eta$ reaches a minimum value of -1, at a particular energy. This causes $\eta \to -\infty$ over a very narrow energy interval. Then $|\sinh\eta|$ is exponentially large, but so is the numerator. Their ratio is of order $e^{-N|\theta|}$ which is small. Given that η is varying extremely rapidly, there will be a nearby energy at which the argument of $\sinh(N\theta + \eta)$ in line four, is zero. If so, because θ is varying slowly compared to η, the position will depend very little on the number of cells N. (If $|\theta|$ is small compared to $|\eta|$, it may require a minimum value of N before such a bound state occurs.) Once it occurs, it will persist in the many-cell situation at almost the same energy. This mechanism allows a bound state to occur in a forbidden zone, unlike the case of transmission resonances which occur only in allowed zones above threshold.

Such bound states decay like $e^{-\kappa x}$ as one moves away from the array, and like $e^{-|\theta|}$ as one moves from cell to cell inside the array. They are the surface states discussed originally by Shockley [15]. We will give examples in section 6.

III. ANALYTICAL EXAMPLE: DIRAC COMB

When the inter-cell distance becomes very large, we should expect each well to behave as an independent system. If a single well has one bound state, the assembly will initially have N degenerate bound states which split as the spacing between the wells decreases. The system properties should depend primarily on two dimensionless parameters. One of these is kd, related to the ratio of cell size to wavelength, and the other is a measure of potential strength to kinetic energy. The simplest example of such a system is the Dirac comb, a line of delta-function potentials. The basic cell is defined on $0 \le x \le d$ with

$$V(x) = -C_0 \delta(x - d/2) \quad . \tag{17}$$

Here we assume $C_0 > 0$ so we have an attractive force, which is opposite to the convention in ref. [1]. In the negative energy region where $k \to i\kappa$, we set

$$\begin{aligned} \kappa^2 &= -\frac{2m}{\hbar^2} E \\ 2\Omega &= \frac{2m}{\hbar^2} C_0 \quad . \end{aligned} \tag{18}$$

Our dimensionless parameters are κd and Ωd.

The transfer matrix for this system is

$$\mathbf{M} = \begin{pmatrix} \frac{\kappa-\Omega}{\kappa} e^{\kappa d} & -0\frac{\Omega}{\kappa} \\ \frac{\Omega}{\kappa} & \frac{\kappa+\Omega}{\kappa} e^{-\kappa d} \end{pmatrix} \tag{19}$$

It is immediately seen that the bound state occurs at $\kappa = \Omega$. (Had we taken a repulsive potential, we would instead have had a virtual state at this energy.) Also, we have

$$\begin{aligned} \cos\phi &= \cosh \kappa d - \frac{\Omega}{\kappa} \sinh \kappa d \\ \frac{1}{2}(M_{11} - M_{22}) &= \sinh \kappa d - \frac{\Omega}{\kappa} \cosh \kappa d \end{aligned} \tag{20}$$

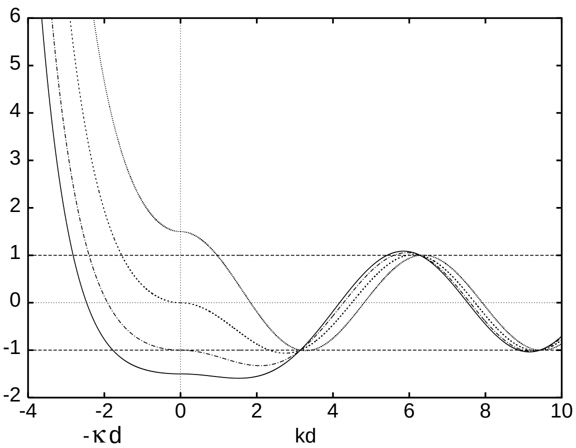

FIG. 1. $\cos\phi$ for $\Omega d = -0.5$ (dotted line), 1.0 (dashes), 2.0 (dot-dash), and 2.5 (solid) for a delta-function potential, plotted against kd above threshold and $-\kappa d$ below threshold.

At threshold ($\kappa \to 0$), $\cos\phi = 1 - \Omega d$. For large enough separation d between the teeth of the comb, this will be less than -1, and threshold occurs in a forbidden zone. Various possibilities are illustrated in Fig. 1, where we plot $\cos\phi$ against kd above threshold, and against $-\kappa d$ below threshold. (So, on the rhs, k runs along the real axis, and on the lhs, up the imaginary axis.) When $\Omega d = -0.5$, we have a repulsive potential, so the first allowed band is entirely above theshold. For $\Omega d = 1.0$, the band is half above and half below threshold. For $\Omega d = 2.0$, the band is entirely below threshold, and as d increases further, it moves increasingly to the left. On the other hand, the second and subsequent allowed bands remain above threshold and their position hardly changes. They are essentially locked in positions with their extreme values at integer multiples of π. That only one allowed band moves below threshold, reflects the fact that a single delta function potential has only one bound state.

For the moment let us consider large Ωd of which the value 2.5 is representative. At the single-cell bound state, $\cos\phi = e^{-\Omega d}$ so one is in an allowed zone, where the forms listed in eq. 19-20 apply. Since Ωd is large, this value of $\cos\phi$ will be very small, giving $\phi \approx \pi/2 - \epsilon$. From eq. 11, $\tan\delta = -\tan\phi \to -\infty$, so $\delta = \pi/2 + \epsilon$. Moving from threshold to negative energy, we enter the allowed zone with $\phi = \delta = \pi$ and we leave it at a point $\kappa > \Omega$ with both angles approaching zero. The bottom of the band corresponds to $\cos\phi = 1$, which implies

$$\begin{aligned} \cosh \kappa d - 1 &= \frac{\Omega}{\kappa} \sinh \kappa d \quad \text{or} \\ \tanh \frac{1}{2} \kappa d &= \frac{\Omega d}{\kappa d} \end{aligned} \tag{21}$$

Since this is in the region $\kappa > \Omega$, a solution exists giving the value of κd, which is always smaller than $2\Omega d$.

Looking at eq. 16, the phase $\chi_N = N\phi + \delta$ ranges from $(N+1)\pi$ to zero over the allowed zone. There will therefore be N bound states of the N-cell system at places where $\chi_N = j\pi$, $j = 1, 2, \ldots N$. For odd-N, one of these will lie very close to the single-cell bound state at $\kappa = \Omega$. In general they are distributed half above and half below this wave number. This situation is again analogous to the occurrence of transmission resonances in an allowed zone above threshold. The number here is N rather than $N - 1$ because the single-cell bound state already occurs within this band.

If Ωd is small, for example 1.0, the single-cell bound state will occur closer to threshold. Part of the allowed band has crossed threshold, leaving less room for bound states of the N-cell system to occur.

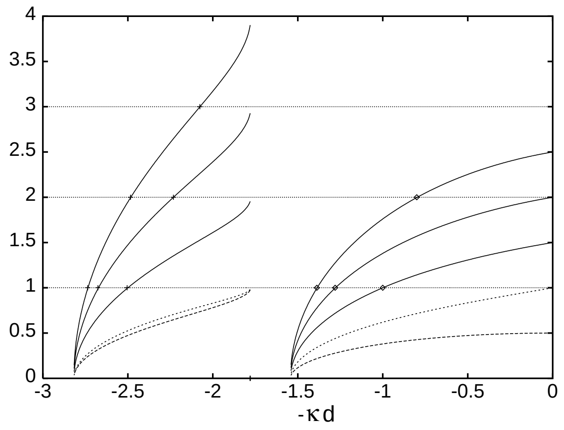

FIG. 2. δ, (short dash line), ϕ, (long dash line) and χ_N for $N = 1, 2, 3$, (solid lines), all divided by π, for two cases: $\Omega d = 2.5$ at left, and 1.0 at right. Bound state positions are marked. Horizontal axis is $-\kappa d$.

In Fig. 2 we have plotted ϕ , δ, and χ_N, (all divided by π), for $N = 1, 2, 3$, for two representative cases discussed above. When $\Omega d = 2.5$, (drawn at left,) $\delta \approx \phi$, as seen at the bottom of the figure. The lines of χ_N/π cross the integers at the N bound states, which are marked. In the other case, $\Omega d = 1.0$, (drawn at right,) ϕ only varies from zero at the zone boundary to $\pi/2$ at threshold, while δ still covers the full range. Then for $N = 2$, $2\phi + \delta$ just reaches 2π at threshold. The second bound state is just barely bound at zero energy, and for $N = 3$, there are only two bound states rather than three. Gasiorowicz [18] discusses the $N = 2$ case in detail and draws the same conclusion. But by adding additional lines in Fig. 2, one can easily locate the states for any N.

IV. ANALYTICAL EXAMPLE: SQUARE WELLS

For the square well, of depth $-V_0$ and width $2b$, we take eq. 32-33 of ref. [1], but revised to correspond to placing the well symmetrically in the centre of the basic cell. Above threshold, with $E = (\hbar^2/2m)k^2$, one has

$$M_{11} = e^{-ik\ell}[\cos 2\gamma b + \frac{k^2+\gamma^2}{2ik\gamma} \sin 2\gamma b] = M_{22}^*$$
$$M_{12} = \frac{k^2-\gamma^2}{2ik\gamma} \sin 2\gamma b = M_{21}^* \tag{22}$$

from which

$$\cos\phi = \cos k\ell \cos 2\gamma b - \frac{k^2+\gamma^2}{2\gamma k} \sin k\ell \sin 2\gamma b \tag{23}$$

As $k \to 0$, we have the limit

$$\begin{aligned}\cos\phi(0) &= \cos 2\gamma b - \frac{\gamma\ell}{2} \sin 2\gamma b \\ &= \cos 2S - \frac{S\ell}{2b} \sin 2S\end{aligned} \tag{24}$$

where as usual [17] $S^2 = 2mV_0b^2/\hbar^2$ is a dimensionless measure of strength for a square well, and $\gamma^2 = (2m/\hbar^2)(E + V_0)$ measures the energy above the bottom of the potential well. At zero energy (threshold), $\gamma b = S$. To compare with the Dirac comb, we let $b \to 0$ while $S^2/b \to 2\Omega$. This makes $\cos\phi(0) = 1 - \Omega\ell$, showing that the inter-well separation ℓ plays the role of d in the Dirac comb result.

For energies below zero, but above the well bottom, $k \to i\kappa$, while γ remains real. The transfer matrix then has elements

$$M_{11} = e^{\kappa\ell}[\cos 2\gamma b + \frac{\kappa^2-\gamma^2}{2\kappa\gamma} \sin 2\gamma b]$$
$$M_{12} = \frac{\gamma^2+\kappa^2}{2\kappa\gamma} \sin 2\gamma b = -M_{21}$$
$$M_{22} = e^{-\kappa\ell}[\cos 2\gamma b - \frac{\kappa^2-\gamma^2}{2\kappa\gamma} \sin 2\gamma b] \tag{25}$$

Then

$$\cos\phi(i\kappa) = \cosh\kappa\ell \cos 2\gamma b + \frac{\kappa^2-\gamma^2}{2\gamma\kappa} \sinh\kappa\ell \sin 2\gamma b\,. \tag{26}$$

The limit value at $\kappa = 0$ is naturally the same as in eq. 24. For strong narrow potentials (large S, small b) the tendency is to have a forbidden band just at threshold, as in the Dirac comb case. However the $\sin 2S$ factor should work against this, reducing the tendency towards large negative values. Moving the energy down to the bottom of the well, κ increases to S/b, while γ decreases to zero. At the bottom,

$$\cos\phi(\gamma = 0) = \cosh\frac{2S\ell}{b} + \frac{S}{2}\sinh\frac{2S\ell}{b} \tag{27}$$

This is positive, and large when ℓ is large, so there will be at least one allowed band below threshold.

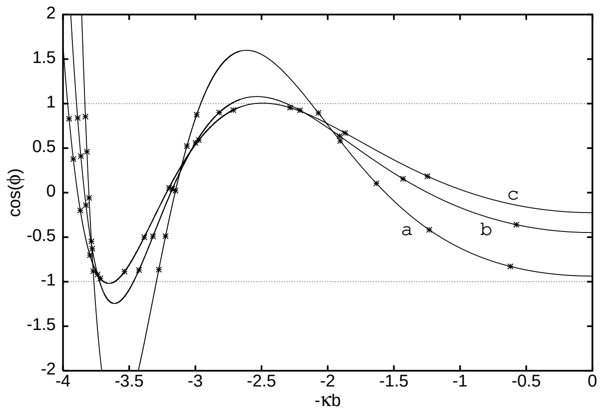

FIG. 3. $\cos\phi$ versus $-\kappa b$ for a square well of strength $S = 4$, for three inter-well spacings (a) $\ell = 4$ nm, (b) 1.53 nm and (c) 0.4 nm. Bound states for $N = 5$ cell system are starred.

Allowed bands are illustrated in Fig. 3 for a case $V_0 = 90$ meV, $2b = 20$ nm (values appropriate for AlGaAs heterostructures) and (a) $\ell = 4$, (b) 1.53 and (c) 0.4 nm. Using $\hbar^2/2m = 0.5625$ eV nm^{-2}, we have $S = 4.00$, so the single well contains three bound states. We plot $\cos\phi$ as a function of $-\kappa b$, which runs from $-S$ (well bottom) to zero (threshold). The asterisks mark the bound state positions for $N = 5$ wells. It is seen that for larger ℓ, the two deep lying bands are very narrow, so the associated N-cell bound states will be almost degenerate for all N. The least bound allowed zone is more spread out. When the wells are placed close together ($\ell = 1.53$ nm), part of this band crosses the threshold, so that for larger N some of the expected N bound states will cross threshold and become unbound (lines b and c). Fig. 4 shows χ_N for these cases and the bound state locations for $N = 1, ...5$. They occur where χ_N/π lines cross the integers. In part (a) we show only two lowest bands in order to use an expanded scale in the drawing.

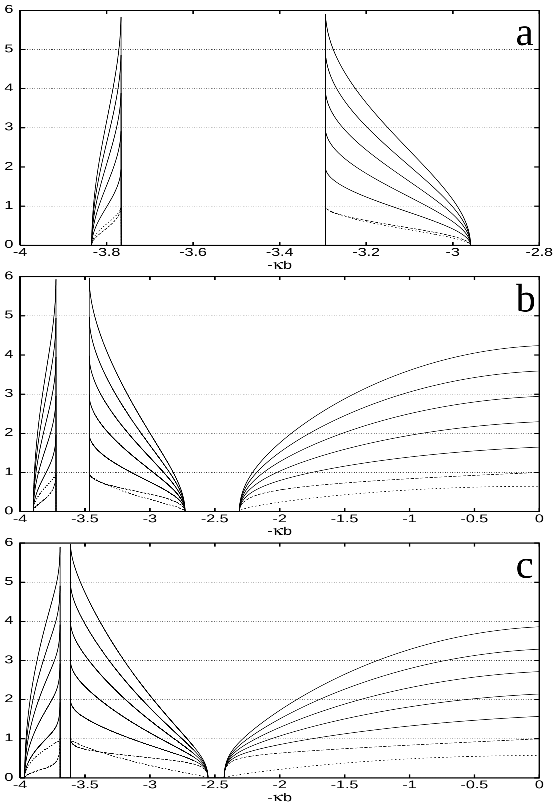

FIG. 4. ϕ, (long dash line) δ, (short dash line) and χ_N for $N = 1, 2, ...5$, (solid lines), all divided by π, for square well potentials of strength $S = 4$, separated by (a) $\ell = 4$, (b) 1.53 and (c) 0.4 nm. Bound states occur where χ_N/π crosses the horizontal integer lines.

A short overview of the bound states for a single well is given in the appendix. For bound states of the N-cell system, we use eq. 16 with the phase δ defined in eq. 11. The denominator involves $M_{11} - \cos\phi = (M_{11} - M_{22})/2$. Now from eq. 25, we see that the exponential factors ensure that generally $|M_{22}| << |M_{11}|$, at least for large $\kappa\ell$. This means that in most situations, the denominator is equal to $\cos\phi$, and therefore $\delta \approx \phi$. To a very good approximation the N-cell bound states are determined by

$$\sin(N\phi + \delta) \approx \sin(N + 1)\phi = 0 \tag{28}$$

with solutions at $\phi_j = j\pi/(N+1)$, $j = 1, 2, ...N$. When N is odd, one of these coincides with the single-cell bound state; otherwise they are evenly split half above and half below this point as functions of ϕ. If ϕ varies linearly with energy then the distribution in energy would also be regular. This is the generic situation for large well separation: for each allowed band below threshold energy, there is one bound state for each well and the states all lie within the band.

When $\kappa\ell$ is small however, one may possibly be in the situation where the orders of magnitude are reversed: $|M_{11}| << |M_{22}|$. Then $\delta \approx \pi - \phi$, so the bound state condition becomes

$$\sin(N\phi + \delta) \approx -\sin(N - 1)\phi = 0 \tag{29}$$

with solutions at $\phi_j = j\pi/(N - 1)$, $j = 1, 2, ...N - 2$. In this case, the phase χ_N runs from π at one end of the band to $N\pi$ at the other end, allowing for only $N - 2$ bound states. The two missing states can then appear in the forbidden zone, one on either side of the allowed zone. It was shown by Shockley [15] that two bands must coalesce and overlap for this to occur. We will discuss such cases in section 6.

V. INTER-WELL SPACING

It is instructive to consider the limit $\ell \to 0$ for the square well. Then increasing N simply makes a square well of fixed depth and larger width Nb. Considered as a single cell, the strength parameter S becomes $S_N = NS$. Suppose, for sake of argument, that initially S is just below $\pi/2$, so that there is only one bound state per well, but one is close to threshold for the second state to occur. Then S_N will be close to $N\pi/2$ and the well will contain N bound states, up to the point where the shortfall of S causes $S_M < (M - 1)\pi/2$. Then for $N = M$, the wide well will contain only $M - 1$ bound states.

Up to that point, the N bound states will be the states in the allowed band provided by the solutions of eqs. A1 from the viewpoint of a single well, or from eq. 28 from the viewpoint of an N-cell system. Obviously the lowest state is nodeless, and the number of nodes increases by one up to the top state with $N-1$ nodes. If we now start to increase ℓ, it is equivalent to putting narrow equally spaced barriers into the wide well, while stretching it out. The wave functions of the bound states will tend to be reduced in size in these barrier zones, but the nodal structure will persist. The least affected state should be the least bound one, as its nodes are evenly distributed and sit over the introduced barriers, tending to stretch out into regions of low amplitude.

Line (c) of Fig. 3 is relevant here, as the inter-cell spacing $\ell = 0.4$ nm is only 2% of the well width $2b = 20$ nm. One notes that as compared to line (a), the two deeply bound bands are much wider, allowing the N lowest states of the N-cell system to approximate the positions of the states of the single wide potential well of width $2Nb + (N-1)\ell$. For example, if $N = 3$, the three lowest states of the wide well have energies in ratio $1:4:9$ and the latter state would have the same energy as the ground state of the narrow well if we could forget about the correction factor for finite well depth, eq. A4. However that factor is $(NS/(NS+1))^2 = 0.852$ as compared to 0.64 for the narrow well, so the energy would be a third higher on this account. Then if we remember also that the wide well can be taken to have a width $6b + 2\ell = 60.8$ nm rather than 60, we bring the energy down by a factor $(60/60.8)^2$ to be just 1.295 higher, in good agreement with the exact value. The third state has its nodes on top of the barriers so should be the least shifted as compared to the equivalent state of the single well.

VI. OVERLAPPING BANDS AND SURFACE STATES

We have seen that when the system consists of square wells, and their spacing ℓ is reduced until they just touch, the forbidden bands shrink until they just disappear. The allowed bands merge into a single band of the resulting wide well. Compare lines (a), (b) and (c) in Fig. 3 to see this evolution. The lowest energy band is associated with the even parity ground state and the next band with the odd parity first excited state of the unit cell.

Placing a repulsive hump in the middle of each well, (and deepening the attractive pockets on each side so as to keep the average depth fixed,) has the effect of pushing up the energy of even parity states while lowering that of odd parity states of the single cell. As a result, the two lowest bands will already touch at some separation $\ell > 0$. Further reducing ℓ causes the forbidden zone to reappear, but it is a special type of zone that results from an overlapping of the neighbouring allowed bands. Shockley [15] showed that this is the situation in which one state from each of the allowed bands can move into the reopened forbidden zone.

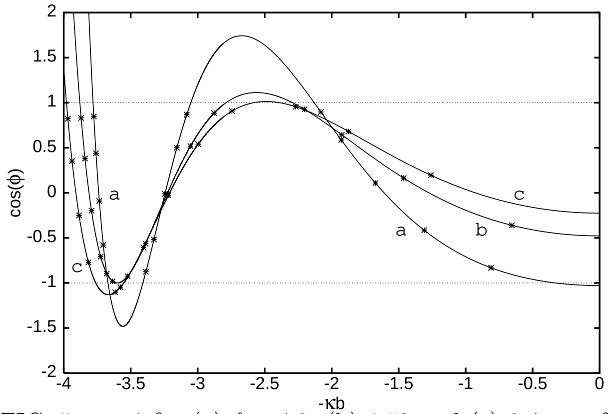

FIG. 5. $\cos\phi$ for (a) $\ell = 4.0$, (b) 1.53 and (c) 0.4 nm, for a square well with a central hump. (Depths -100 and -80 meV.) The two lowest bands overlap for $\ell < 1.5$ nm, allowing surface states to occur.

An example is shown in Fig. 5, where we have taken a unit cell with a central portion of depth 80 meV and width 10 nm; and the wings, 100 meV deep and width 5 nm. on each side. (The potential shape is shown under the wave function in Fig. 8 below.) For $\ell = 4$ nm the bands are distinct; they just touch when $\ell = 1.53$ nm and for $\ell = 0.4$ nm an appreciable forbidden band has reopened. Since the unit cell has reflection symmetry, so does the system of N cells.

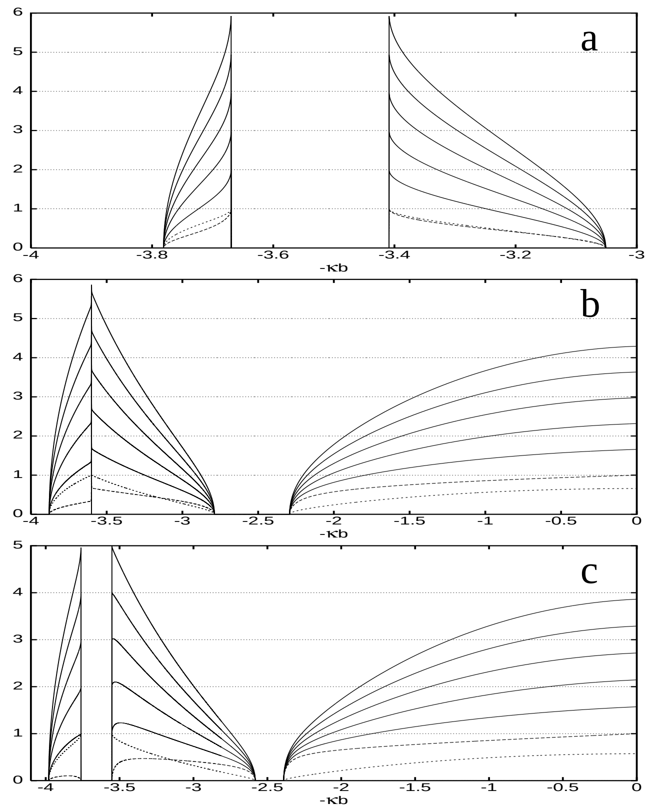

FIG. 6. δ, (short dash line) ϕ, (long dash line) and χ_N for $N = 1, 2, ...5$, (solid lines), all divided by π, for same unit cell as Fig. 5, separated by (a) $\ell = 4$, (b) 1.53 and (c) 0.4 nm. Allowed zone bound states occur where χ_N/π is an integer.

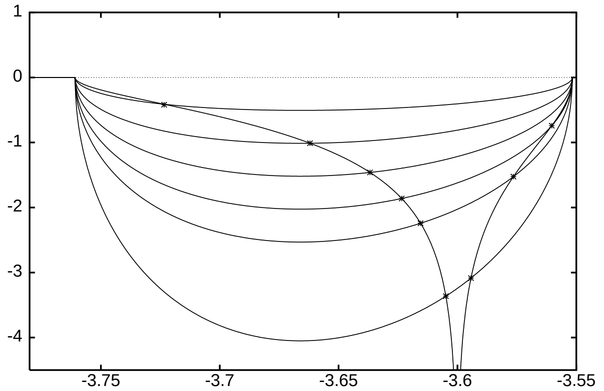

FIG. 7. $N\theta$ for $N = 1...5$ and 8 (from top to bottom) and $-\eta$ (singular line) in the lowest forbidden band, for $\ell = 0.4$ nm. Intersections giving the surface states for the N-cell system are starred.

When $\ell = 4$ nm the bound states are located within the allowed bands, similar to the situation in Figs. 3 and 4. When $\ell = 0.4$ nm we see in Fig. 6 that δ starts and ends with the value zero, and this permits just $N - 1$ bound states in the allowed zone. As a result, some of the bound states have migrated to the forbidden band. (In part (a), only the two lowest bands are drawn, to allow an expanded scale. In cases (b) and (c) the third band overlaps threshold so some of the expected N states have become unbound.)

Fig. 7 is a plot of $-\eta$ and $N\theta$ for $N = 1, 2, ...5$ in the lowest forbidden zone. The intersections give the positions of the surface states, according to eq. 14. For $N = 1$ only the state originating from the ground band has become a surface state; but by $N = 4$ a second state, from the first excited band, has appeared in the gap. Because $\tanh\eta$ has a maximum of unity near $\kappa b = 3.6$, the curve for $-\eta$ descends to $-\infty$ and then rises again. The two states occur one on either side of the singularity. As N increases they approach each other more and more closely. The line for $N = 8$ shows this nicely.

Some surface state wave functions (squared) are shown in Fig. 8. For N cells, it is the N'th and $(N+1)$'st states that become surface states. The reflection symmetry of the array produces wave functions of good parity, so they have large amplitude on both ends of the array. Because $|\theta|$ never becomes very large in this example, for $N = 5$ (inset) the states show only a tendency to surface peaking, while for $N = 20$ it becomes convincing.

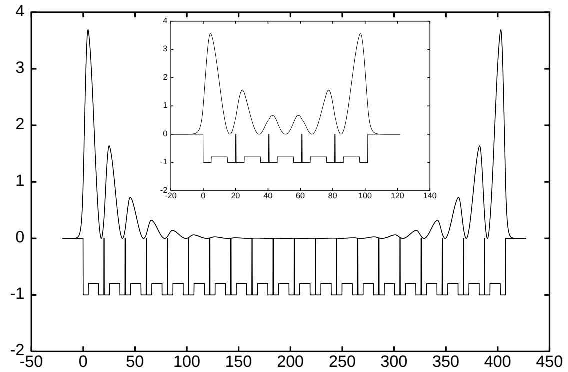

FIG. 8. Squared wave function of the lowest energy surface state for $N = 20$ cells. Inset: same for $N = 5$ cells.

Kalotas and Lee [9] have also considered bound states within the transfer matrix formalism. Among many differences from our work, they take the potential energy outside the array to be infinite, rather than zero. This has the result that within an allowed band, the angle δ of eq. 10 is zero, and there are always just $N - 1$ states which are solutions of $\sin N\phi = 0$. The other bound state occurs in the next forbidden band (or at the band edge), and is built on the bound state of the single cell. Therefore its position is independent of the number of cells N. To see this, suppose that $w(x)$ is the wave function of this state within the unit cell. Let $w(0) = w(d) = 0$, $w'(0) = 1$, $w'(d) = -\beta$, Then in the second cell of an array, the wave function is $\psi(x + d) = -\beta w(x)$, and in the $(k+1)$'th cell, $\psi(x+kd) = (-\beta)^k w(x)$. So if $|\beta| > 1$, the N-cell state will be a surface state strongly concentrated at the far right of the array and if $|\beta| < 1$, it will be peaked at the left edge. Such surface peaked states arise due to the parity asymmetry of the unit cell, and are Tamm type surface states, as Shockley pointed out [15]. When the unit cell has reflection symmetry, then the wave function $w(x)$ has definite parity, so $\beta = \pm 1$. The N-cell state will then have uniform amplitude across all cells. This illustrates the fact that surface states are much harder to find when dealing with parity conserving potentials.

As noted by Kalotas and Lee, this division of the bound states into two groups of $N - 1$ and one, is the analogue of the situation for scattering resonances, as discussed following eq. 8. By taking the external potential to be infinite, they have effectively discretized the continuum, so this is not surprising. Our formalism can be adapted to this situation. If there is a non-zero potential outside the array, then in place of the boundary condition $\psi'/\psi = \pm\kappa$ at the edges, one has some other value $\sigma(\kappa)$. The limit $\sigma \to \infty$ leads to their result, but finite values can be handled just as easily.

VII. SUMMARY AND CONCLUSION

The transfer matrix method relates solutions of the wave equation on opposite sides of a potential cell. We have applied this method to find the bound states of an N-cell system in terms of the Bloch phase and an additional scattering phase δ, in the sub-threshold region. These phases are properties of the single cell.

The important equations are 10 and 12, (14, and 16), depending on whether one is looking in an allowed band (where the Bloch phase ϕ is real), or in a forbidden band. Fig. 2 illustrates how eq. 12 determines the N-cell bound states when they occur in an allowed zone. Similarly, Fig. 7 shows how eq. 14 governs the appearance of surface states.

When the inter-cell distance ℓ is very large compared to the effective range of the potential inside the cell, one is in the situation $|M_{11}| >> |M_{22}|$, which leads to $\delta \approx \phi$. Then the number of bound states in the allowed band will be N, and they are uniformly spread across the band with the $N = 1$ state being at the band center. This is the generic situation: the N states are linear combinations of the states where the particle is trapped in a single well. However, when ℓ is small, some of these states may cease to be bound, as we saw in the soluble example of the square well.

Many text books discuss the double square well as an example of the splitting of a pair of bound states. The presentation of the wave function matching is straightforward but tedious. We think that the present formalism, which allows one to discuss N-cells with no more effort than a single cell, gives better insight into the general principles. It also allows one to discuss the situation qualitatively while avoiding detailed calculations.

ACKNOWLEDGMENTS

We thank Prof. Tim Londergan for asking the question that brought us to reconsider the bound state problem. We are grateful to DGES, Spain for continued support through grant PB97-0915 (JM), and to NSERC Canada for research grant SAPIN-3198 (DWLS), and a Summer Research Assistantship (JDS). This work was carried out as part of CERION, an Esprit project EP-27119 funded by the EU.

APPENDIX A: SQUARE WELL BOUND STATES

The bound states of the single-cell are determined by

$$M_{11} = 0 = e^{\kappa\ell}\left[\cos 2\gamma b + \frac{\kappa^2 - \gamma^2}{2\kappa\gamma}\sin 2\gamma b\right] \quad . \tag{A1}$$

This is satisfied only when the quantity in square brackets is zero, independently of ℓ as it must be. Since $\gamma^2 + \kappa^2 = S^2/b^2$, we may write $\gamma b = S \sin\theta_a$ and $\kappa b = S\cos\theta_a$. (θ_a is just an auxiliary symbol not related to anything used before!) Then we have

$$\begin{aligned} \sin 2\theta_a \cos 2\gamma b + \cos 2\theta_a \sin 2\gamma b = 0 \quad \text{or} \\ \sin(2\theta_a + 2\gamma b) = 0 \quad . \end{aligned} \tag{A2}$$

This is satisfied when the argument is an integer multiple of π, giving

$$\begin{aligned} \gamma b = S\sin\theta_a = S\sin(n\pi/2 - \gamma b) \quad \text{or} \\ \frac{\gamma b}{S} = \sin(n\pi/2 - \gamma b) \quad n = 1, 2, \cdots \end{aligned} \tag{A3}$$

The solution of eq. A3 is the method for finding bound states discussed by us in earlier works: [16,17], and corresponds to the Pitkanen construction [19]. Counting the states from $n = 1$, the condition for the n-th bound state to exist is $S \geq (n-1)\pi/2 \equiv c_n$. When S is large, the line of slope $1/S$ intersects a loop of a sine curve (peak at c_n) near a node at c_{n+1}; if we approximate the sine by its tangent $y = n\pi/2 - \gamma b$, then the intersection is at

$$\gamma_n \approx \frac{n\pi}{2b}\frac{S}{S+1}(1+\cdots) \quad , n = 1, 2, \ldots \tag{A4}$$

Since γ is the wave number measured from the bottom of the potential well, the bound state energy is, to leading order, a fraction $(S/S+1)^2$ of the energy of the corresponding state of the infinitely deep square well. It lies below because the edge of the finite well is less repulsive than the deep well. (For weakly bound states another approximation is available; see [16].)

[1] D.W.L. Sprung, Hua Wu and J. Martorell, "Scattering by a Finite Periodic Potential", Am. J. Phys. **61** (1993) 1118-24.

[2] R. de L. Kronig and W.G. Penney "Quantum Mechanics of Electrons in Crystal Lattices", Proc.Roy.Soc. (London) **A130**, 499-513 (1931).

[3] J.A. Brum, "Electronic properties of quantum-dot superlattices" Phys. Rev. B, **43** (1993) 12082-5.

[4] David Kiang "Multiple Scattering by a Dirac Comb", Am.J.Phys. **42**, 785-7 (1974).

[5] D.J. Vezzetti and M. Cahay, "Transmission Resonances in Finite Repeated Structures", J. Phys. D (Applied Phys.) **19** , L53-55 (1986).

[6] S.E. Ulloa, E.Castaño, and G. Kirczenow, "Ballistic Transport in a Novel One-dimensional Superlattice", Phys.Rev.B **41**, 21350-3 (1990).

[7] Hua Wu, D.W.L. Sprung, J. Martorell and S. Klarsfeld, "Quantum Wire with Periodic Serial Structure", Phys. Rev. B **44**, 6351-60 (1991).

[8] T.M. Kalotas and A.R. Lee, "One-dimensional Quantum Interference", Eur.J.Phys. **12**, 275-82 (1991).

[9] T.M. Kalotas and A.R. Lee, "The spectra of periodic potentials in finite boxes", Eur.J.Phys. **16**, 119-123 (1995).
[10] D.J. Griffiths and N.F. Taussig, "Scattering from a Locally Periodic Potential", Am.J.Phys. **60**, 883-8 (1992).
[11] R. G. Newton, "Comment on 'Scattering by a Finite Periodic Potential'", Am. J. Phys. **62** (1994) 1042-3.
[12] S.J. Blundell, "The Dirac Comb and the Kronig-Penney Model; Comment on 'Scattering from a Locally Periodic Potential'", Am.J.Phys. **61**, 1147 (1993).
[13] C. Cohen-Tannoudji, B. Diu and F. Laloë, "Quantum Mechanics", Wiley, N.Y., (1977), Vol. 1, pp. 367-383.
[14] Hua Wu, D.W.L. Sprung and J. Martorell, "Periodic quantum wires and their quasi-one-dimensional nature" J. Phys. D**26**, 798-803 (1993).
[15] W. Shockley, "Surface states associated with a periodic potential", Phys. Rev. **59** (1939) 319-323.
[16] D.W.L. Sprung, Hua Wu and J. Martorell, "A New Look at the Square Well Potential", European J. Phys. **13** (1992) 21-25.
[17] D.W.L. Sprung, Hua Wu and J. Martorell, "Poles, Bound States and Resonances illustrated by the finite square well potential", Am. J. Phys. **64** (1996) 136-144.
[18] S. Gasiorowicz, "Quantum Mechanics", Wiley, N.Y., (1974), pp. 93-98.
[19] P.H. Pitkanen, "Rectangular potential well problem in quantum mechanics", Am. J. Phys. **23** (1955) 111-113.

file: d:/n99/shock/boundrv.tex